Global Energy Interconnection
Development and Cooperation Organization

ELSEVIER
Production And Hosting By Elsevier On Behalf Of KeAi
KeAi

Volume 3 Number 4 August 2020 (346-354)
DOI: 10.14171/j.2096-5117.gei.2020.04.005

Global Energy Interconnection

Contents lists available at ScienceDirect
https: //www.sciencedirect.com/journal/global-energy-interconnection

Full-length article

Generation-expansion planning with linearized primary frequency response constraints

Zihan Wang, Jianxiao Wang, Gengyin Li, Ming Zhou
School of Electrical and Electronic Engineering, North China Electric Power University, Beijing 102206, P.R. China

Scan for more details

Abstract: As renewable energy resources increasingly penetrate the electric grid, the inertia capability of power systems has become a developmental bottleneck. Nevertheless, the importance of primary frequency response (PFR) when making generation-expansion plans has been largely ignored. In this paper, we propose an optimal generation-expansion planning framework for wind and thermal power plants that takes PFR into account. The model is based on the frequency equivalent model. It includes investment, startup/shutdown, and typical operating costs for both thermal and renewable generators. The linearization constraints of PFR are derived theoretically. Case studies based on the modified IEEE 39-bus system demonstrate the efficiency and effectiveness of the proposed method. Compared with methods that ignore PFR, the method proposed in this paper can effectively reduce the cost of the entire planning and operation cycle, improving the accommodation rate of renewable energy.

Keywords: Frequency equivalent model, Generation expansion planning, Inertia, Primary frequency response.

1 Introduction

In recent years, the continually increasing development and utilization of renewable energy has made the integration of wind power into the grid a major issue in power-generation system development. However, due to the complete decoupling of mechanical power and system electromagnetic power in a variable-speed constant-frequency (VSCF) wind turbine, and the consequent decoupling of rotor speed and system frequency, the wind turbine has little inertial response [1][2]. To solve the problem of providing adequate primary frequency response (PFR) in the power system, it is essential to incorporate PFR constraints in the generation-expansion planning stage.

An abnormal frequency will seriously affect the steady operation of a power system; when the frequency deviates greatly, the system will respond. Among the various stages of response to a frequency transient, PFR is the fastest: the governors' response time is on the order of seconds to prevent further deviations in frequency [3][4]. The frequency nadir, reflecting the maximum deviation of frequency, will appear during the PFR phase [5]. For these reasons, this paper takes PFR as the main compensatory measure for large and sudden outages.

The most important methods used to analyze the dynamic frequency response of a power system to a disturbance are the time-domain simulation method [6] and the equivalent-model method [7][8][9][10][11]. The time-domain simulation method is highly accurate but entails complex calculations; it is difficult to use in modeling. The

Received: 16 May 2020/ Accepted: 5 July 2020/ Published: 25 August 2020

✉ Jianxiao Wang
wangjx@ncepu.edu.cn

Gengyin Li
ligy@ncepu.edu.cn

Zihan Wang
wangzh@ncepu.edu.cn

Ming Zhou
zhouming@ncepu.edu.cn

equivalent-model method simplifies the power system to a single-unit single-load model; it can be nearly as accurate as dynamic simulation at a more reasonable calculation cost. Through a series of simplifications and by highlighting the main influencing factors, a system-frequency response model is established in [7], but the analytical form of the frequency response is highly non-linear, and it is difficult to find an explicit linear approximation. The authors of [8] propose linear constraints on PFR suitable for an optimal power flow (OPF) framework and clearly define the concept of the governor reserve, but the impact of the load damping rate is not considered. A method to calculate the maximum frequency deviation using the governor-model approximation and a frequency feedback loop is presented in [9], but load variation with frequency is neglected. Linearized PFR constraints are incorporated into power system scheduling in [10], taking the PFR capacity and ramp rate requirement into account. A novel mixed-integer linear programming (MILP) formulation for system frequency constraints is presented in [11]; it ensures that the post-fault frequency deviation remains within limits. However, the effect of the ratio of maximum primary reserves to the generator capacity is not analyzed. Moreover, the proposed MILP formulation is only applied to security-constrained economic dispatch or unit commitment during the operation stage, not to the impact of PFR on generation planning.

In practice, few existing studies and projects have considered the requirements for system-wide PFR when making planning decisions. Without such consideration, a system operator will tend to over-invest in renewable energy resources, while the total delivery of PFR may be reduced in real time, leading to renewable production curtailment. We therefore incorporate linearized PFR constraints into a collaborative planning model of thermal power and renewable energy and develop an optimal generation-expansion planning framework. Our major contributions are the following:

(1) An optimal generation-expansion planning framework for a power system is proposed considering the PFR requirement. As an MILP formulation, this framework can coordinate the expansion of renewable and conventional generation, thereby ensuring security of real-time operation and avoiding over-investment in renewable energy resources.

(2) An equivalent model of PFR is formulated to keep the frequency deviation within limits, considering the impact of the load damping rate. This equivalent model includes a series of linearization formulas for the frequency nadir and the limits of primary reserves for governor use.

2 Primary frequency response model

This section proposes the equivalent model of frequency evolution, formulates the limits of primary reserves for governor use, and linearizes the constraints of the maximum allowable frequency deviation.

2.1 Equivalent model of frequency evolution

At present, the power supply of a power system is composed mainly of thermal power units. The whole power system is equivalent to a single generator, and its PFR equivalent machine model is shown in Fig. 1.

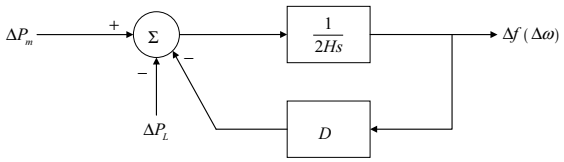

Fig. 1 Equivalent model of power system

The fundamental single-machine model of the frequency evolution process can be expressed as [12]

$$\Delta P_m - \Delta P_e = 2H \frac{d\Delta\omega}{dt} \tag{1}$$

where ΔP_m represents the mechanical power deviation, ΔP_e is the electromagnetic power deviation, H refers to the system inertia, and $\Delta\omega$ means the rotor speed deviation.

In general, the power system load is a series of electrical devices, including both frequency-insensitive and frequency-sensitive ones. The electromagnetic power deviation can be expressed as

$$\Delta P_e = \Delta P_L + D\Delta\omega \tag{2}$$

where ΔP_L is the frequency-insensitive load change, and $D\Delta\omega$ is the frequency-sensitive load change [13]. Note that D is the load damping rate, which can be expressed as the percentage change in load caused by a 1% deviation of frequency; it is introduced into the model to reflect how the load regulates the power system frequency [14][15]. The velocity ω of the equivalent machine represents the frequency of the system. When the per-unit value system is used, the system frequency deviation Δf is equal to $\Delta\omega$.

Equation (1) can be converted into

$$\Delta P_m - \Delta P_L = 2H \frac{d\Delta f}{dt} + D\Delta f \tag{3}$$

The first-order differential equation (3) expresses the dynamics of system frequency deviation. The main parameters affecting frequency deviation are the system inertia and the load damping rate. Assuming that wind power cannot provide inertia for the system, the inertia of the system [16][17] can be expressed as

$$H = \sum_{g\in\Phi^{CG}} \frac{P_{g,\max}}{S_B}\alpha_g^{CG} x_{g,t} H_g \tag{4}$$

where $P_{g,\max}$ is the nominal power of thermal generator g; H_g is the inertia constant of generator g; S_B is the base power of system; the binary variable α_g^{CG} indicates whether the conventional generator g is included in the construction plans; and the binary variable $x_{g,t}$ indicates whether thermal generator g is online in time slot t.

By analyzing the time-dependent relationship between the generator output regulated by the governor and the system frequency in the actual response stage, the former can be expressed as a piecewise linear function of the frequency [8]. Such piecewise linearization of the governor model makes it convenient to incorporate the PFR constraints into the planning and design of the power system. The total delivery of PFR in the power system is then given by

$$\Delta P_m = \begin{cases} 0, & 0 < t < t_{DB}, \\ \dfrac{R}{T_d}\left(t - t_{DB}\right), & t_{DB} \leqslant t \leqslant T_d + t_{DB}, \\ R, & t > T_d + t_{DB}. \end{cases} \tag{5}$$

where T_d is the delivery time of PFR, less than 10 s according to the present British practice [18]; R means the total PFR provision from thermal power units [19] [20]; and t_{DB} is the dead-band, which prevents the governor from excessively reacting to small and frequent frequency changes [21][22]. At the same time, since the existence of dead-bands will delay the response speed of the governor, appropriately reducing the dead-band time will improve the PFR of the system.

By integrating (3) and denoting t-t_{DB} by t', the frequency deviation Δf during the PFR phase ($t \leqslant T_d + t_{DB}$) can be expressed as

$$\Delta f = \begin{cases} \dfrac{\Delta P_L}{D}\left(e^{-\frac{D}{2H}t} - 1\right), & 0 < t < t_{DB}, \\ \Delta f_{DB} + \dfrac{1}{D}\left(\dfrac{2HR}{T_d D} + \Delta P_L\right)\left(e^{-\frac{D}{2H}t'} - 1\right) & \\ + \dfrac{R}{DT_d}t', & t_{DB} \leqslant t \leqslant T_d + t_{DB}, \end{cases} \tag{6}$$

where Δf_{DB} means frequency dead-band. The total frequency response provision of system R satisfies

$$R = \sum_{g\in\Phi^{CG}} R_{g,s,t} \tag{7}$$

where $R_{g,s,t}$ is defined as the primary reserve from unit g for governor use; it is distributed among the different participant generators in primary frequency response [23]. The primary reserve $R_{g,s,t}$ and the scheduled generation $P_{g,s,t}^{CG}$ for an arbitrary unit g under scenario s in time slot t satisfy

$$0 \leqslant R_{g,s,t} \leqslant \alpha_g^{CG} x_{g,t} R_{g,\max} \tag{8}$$

$$R_{g,s,t} + P_{g,s,t}^{CG} \leqslant \alpha_g^{CG} x_{g,t} P_{g,\max}^{CG} \tag{9}$$

where $R_{g,\max}$ is ramp-up limit under primary regulation, namely the maximum primary reserve of unit g.

A necessary (but not sufficient) condition [8] for the system to regulate post-fault frequency deviation within limits is that the sum of primary reserves from all thermal units be larger than the largest possible loss:

$$\sum_{g\in\Phi^{CG}} R_{g,s,t} \geqslant P_{loss} \tag{10}$$

where P_{loss} means a sudden loss of power generation, especially the loss of maximum power of any single generating unit, and, in this case, ΔP_L is equal to the negative value of P_{loss}.

2.2 Linearized formulation for the frequency nadir

After sudden, large disturbances, such as the loss of the unit with the largest capacity, the minimum frequency (the "frequency nadir") exists during the primary frequency response phase. The frequency nadir meets the condition of $\partial\Delta f/\partial t$=0, then the time t^* satisfies:

$$t^* = t_{DB} - \frac{2H}{D}\ln\frac{2HR}{2HR + DT_d\Delta P_L} \tag{11}$$

The deviation of the frequency nadir can be expressed as

$$\Delta f_{nadir} = \Delta f_{DB} - \frac{\Delta P_L}{D} - \frac{2HR}{D^2 T_d}\ln\frac{2HR}{2HR + DT_d\Delta P_L} \tag{12}$$

where HR corresponds to the square of the energy provided by the governor to keep the system unit running at the original speed, denoted by z; $DT_d\Delta P_L$ corresponds to the product of the energy change generated by the frequency-insensitive load change with the fluctuation value of the load-demand energy caused by the frequency change during the PFR stage, denoted by A; $\Delta P_L/D$ corresponds to the change in frequency caused directly by the load change, depending on the load damping, denoted by Δf_D.

The frequency deviation should not exceed the predefined threshold:

$$\left|\Delta f_{nadir}\right| \leqslant \left|\Delta f_{\max}\right| \tag{13}$$

According to (12) and (13), the deviation of the frequency nadir is limited by

$$\frac{2z}{A}\ln\frac{2z}{2z + A} \leqslant \frac{1}{\Delta f_D}\left(\Delta f_{\max} + \Delta f_{DB} - \Delta f_D\right) \tag{14}$$

The left side of the inequality is a monotonically decreasing function of z. The equation can be established if and only if z=z^*. z^* satisfies:

$$\frac{2z^*}{A}\ln\frac{2z^*}{2z^* + A} = \frac{1}{\Delta f_D}\left(\Delta f_{\max} + \Delta f_{DB} - \Delta f_D\right) \tag{15}$$

According to monotonicity, $z \geqslant z^*$. In addition, considering $z=HR$ and (4), although z is formulated into an explicit form, the relational expression contains the nonlinearity. Considering the constraint imposed by the unit planning variable α_g^{CG} on the unit state variable $x_{g,t}$, and denoting the product $x_{g,t}R$ by a new continuous variable $y_{g,t}$, the following mixed integer linear constraints are satisfied:

$$\frac{\sum_{g\in\Phi^{CG}} H_g P_{g,\max} y_{g,t}}{S_B} \geqslant z^*, \forall t, \tag{16}$$

$$R - M\left(1-x_{g,t}\right) \leqslant y_{g,t} \leqslant R + M\left(1-x_{g,t}\right), \forall g,t, \tag{17}$$

$$-Mx_{g,t} \leqslant y_{g,t} \leqslant Mx_{g,t}, \forall g,t, \tag{18}$$

$$R = \sum_{g\in\Phi^{CG}} R_{g,s,t}, \forall s,t, \tag{19}$$

$$0 \leqslant R_{g,s,t} \leqslant x_{g,t} R_{g,\max}, \forall g,s,t, \tag{20}$$

$$R_{g,s,t} + P_{g,s,t}^{CG} \leqslant x_{g,t} P_{g,\max}^{CG}, \forall g,s,t, \tag{21}$$

$$\sum_{g\in\Phi^{CG}} R_{g,s,t} \geqslant P_{loss}, \forall s,t, \tag{22}$$

$$x_{g,t} \leqslant \alpha_g^{CG}, \forall g,t. \tag{23}$$

where M is a large number. Constraints (16), (17), and (18) give the limits of the frequency nadir. Constraints (19), (20), (21), and (22) show the limits of primary reserves in the power grid. Constraints (23) show the limit of the unit state variable $x_{g,t}$ imposed by the unit planning variable α_g^{CG}.

3 Optimal planning model

In this section, an optimal generation-expansion planning model of a power system with load growth is proposed, taking into account the PFR constraints. Considering the uncertainties on both the supply and demand sides, including the uncertainties in wind-power output and demand for power, the model requires stochastic optimization [24].

The different power-supply components in the power-generation plan will have different service lives, and therefore different remaining service lifetimes at the end of the planning year. Our model deals with this part of the residual value by using the uniform annual value. The objective function being minimized is the expected uniform annual value C_e consisting of the total cost of planning and operation for all scenarios. The problem of finding the optimal planning strategy is formulated as follows:

$$\min C_e = C_p + C_o \tag{24}$$

$$C_p = \sum_{g\in\Phi^{CG}} \alpha_g^{CG} C_g^{CG} \beta_g + \sum_{r\in\Phi^{RG}} \alpha_r^{RG} C_r^{RG} \beta_r \tag{25}$$

$$C_o = \sum_{s\in\Phi^S}\sum_{t\in\Phi^T}\sum_{g\in\Phi^{CG}} \gamma_s \left(k_g^{CG} P_{g,s,t}^{CG} + c_g^U U_{g,t} + c_g^D V_{g,t}\right) - \sum_{s\in\Phi^S}\sum_{t\in\Phi^T}\sum_{r\in\Phi^{RG}} \gamma_s \mu^{RG} P_{r,s,t}^{RG} \tag{26}$$

$$\beta_i = \frac{r^D\left(1+r^D\right)^{N_i^L}}{\left(1+r^D\right)^{N_i^L}-1} \tag{27}$$

where C_p and C_o are the uniform annual values of generation planning and actual operation, respectively; C_p is the uniform annual investment cost in conventional (thermal) generators and renewable energy sources; C_o is the uniform annual operating cost of thermal power units (including the start-up, shut-down, and running generation costs) and the annual subsidy of wind power generation.

In the objective function, Φ^S, Φ^T, Φ^{CG} and Φ^{RG} are the sets of scenarios, time slots, thermal generators, and renewable generators, respectively; γ_s refers to the probability of scenario s. In the planning stage, the binary variable α_g^{CG} indicates whether or not the conventional generator g is included in the construction plans; the binary variable α_r^{RG} means whether or not the renewable generator r is included in the construction plans; β_i is the annual average coefficient of the fixed construction-investment cost of generator i; r^D is the discount rate [25]; N_i^L is the service life of the newly constructed generator i; C_g^{CG} and C_r^{RG} are the construction costs of thermal generator g and renewable generator r, respectively. The decision variables in the operation stage are the thermal generators' power $P_{g,s,t}^{CG}$, the renewable power $P_{r,s,t}^{RG}$, and the thermal generators' startup/shutdown variables $U_{g,t}/V_{g,t}$; k_g^{CG}, c_g^U and c_g^D are the generation cost, startup cost and shutdown cost of thermal generator g; μ^{RG} is the unit subsidy for renewable energy production. The objective is to minimize the total costs of planning and operation.

The framework in this paper linearizes this problem so that it becomes an MILP problem, thereby permitting PFR constraints to be included in generation-expansion planning. This framework considers not only PFR constraints, the power-flow limits for lines, and security-constrained unit commitment (SCUC) during the operation stage, but also constraints of primary reserves from units participating in frequency regulation. The full constraints of the generation-expansion planning model are elaborated in the Appendix.

4 Case study

Case studies were performed using MATLAB R2016a and CPLEX 12.4 [27] on a computer with 2.40 GHz CPU and 16 GB RAM. The modified IEEE 39-bus system (Fig. 2) with 24-hour time slots was the grid used for the case

studies. From a security perspective (e.g., the N-1 security criterion), the adequate provision of PFR ensures that, after a contingency, the system frequency is maintained above the frequency threshold.

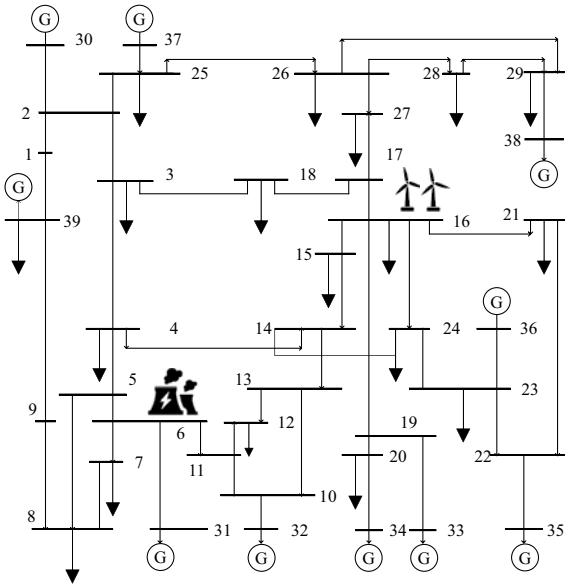

Fig. 2 Structure of the modified IEEE 39-bus system

4.1 Data description

The existing types of conventional generators in the system are shown in Table 1; the number of units of types A, B, C, and D is 1, 2, 3, and 4, respectively. Because of increased power demand, the installed capacity needs to be increased. The plan is to build conventional thermal generators and wind turbines at nodes 6 and 16, respectively, because the load demand near these two nodes is large, and the location distribution of the two nodes can balance the system power more reasonably. The thermal generators to be built are selected from the units provided in Table 1. Suppose the wind turbine has no capability to provide inertial response or primary reserves for governor use, when power expansion planning is carried out. The capacity of a single wind turbine is 1 MW; the construction cost is 1.3 M$, and the maximum planned capacity of the wind farm is 800 MW.

Table 1 Parameters of 4 types of thermal power units

Unit	Capacity (MW)	Cost of construction(M$)	Cost of coal consumption ($/MWh)
A	300	204	20
B	450	300	9.8
C	600	378	10.7
D	900	546	13.9

The wind power and load profiles are collected from the PJM market in the U.S. [28][29]. Fig. 3 shows the output of a 1 MW wind turbine and the system-load data under 10 daily scenarios selected from yearly data by k-means clustering. It is assumed that all thermal generators have a service life of 10 years, a frequency dead-band at 15 mHz, a delivery time of 5 s, and an inertia constant (the same for all generators) of 5.5 s. The maximum primary reserve ratio of unit nominal capacity for each thermal generator is 20%. The service life of a wind turbine is 11 years. The allowed maximum frequency deviation by the system is set to 0.5 Hz.

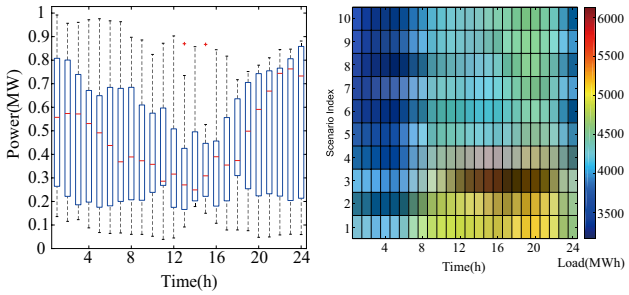

Fig. 3 (left) One-megawatt wind turbine: Power output over time; (right) System load under ten scenarios

To demonstrate the effectiveness and benefits of the proposed generation-expansion planning framework, three methods are compared in the case studies:

(1) M1 is the method proposed in this paper, considering PFR constraints in both the planning and operation stages;

(2) M2 is the currently prevalent planning method, in which PFR constraints are not considered in the planning stage;

(3) M3 is a benchmark, in which PFR constraints are not considered even in the operation stage.

4.2 Optimal planning strategy

Data concerning optimal generation-expansion planning methods are shown in Fig. 4. In M1, construction of one B thermal power unit and 356 1 MW wind turbines is planned, with a wind accommodation rate of 88.05%. In M2, construction of one B thermal power unit and 800 1 MW wind turbines is planned, with a wind accommodation rate of 83.39%. Because M3 is not limited by PFR in either the planning or the operation stage, it adopts the same planning strategy as M2: one B thermal power unit and 800 1 MW wind turbines.

Because it does not consider PFR in the planning stage as M1 does, M2 invests an extra 444 MW in wind turbines; the total cost of M2 is 4.35 M$ more than that of M1. Due

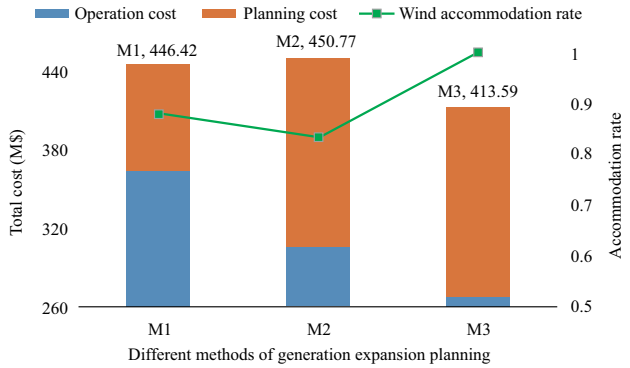

Fig. 4 Market revenues and accommodation rates for three methods of generation-expansion planning

to the smaller wind-power ratio in the generation output, the operational cost of M1 is more than those of the others. The operational cost of M3, which ignores PFR, will be as low as 267.39 M$, and the expected equivalent annual value of its total cost will be 413.59 M$, far less than the total cost of M1. Moreover, M3's wind accommodation rate will reach a satisfactory level close to 1. Although M3 has the least total cost among the three methods, it fails to ensure real-time reliability, because it may be unable to deliver adequate PFR.

Fig. 5 demonstrates the link between the frequency threshold and system frequency nadirs after a contingency for all three methods under 10 daily scenarios in the operation stage. M1 and M2 take the PFR constraints into account so that the power system can ensure primary response adequacy with the frequency nadir above threshold. Without any measure to restrain the scale of wind power integration and to maintain a certain number of thermal generators online, M3 will have a post-contingency frequency nadir in the operation stage that exceeds the predefined threshold.

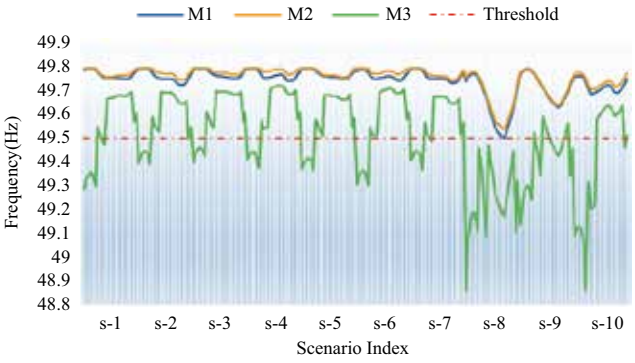

Fig. 5 System frequency nadirs after a contingency for the three methods under 10 daily scenarios

In actual operation, considering the real-time balance of system power and SCUC, excessive penetration of wind power will force thermal generators out of operation. Therefore, it is necessary to restrain the penetration of the 800 MW wind turbines and to maintain the number of online thermal generators in M2. With the grid connection of the wind turbines reduced, the wind-power accommodation rate is only 83.39%, which means 16.61% of wind power cannot be accommodated in the initial strategy. Renewable resources will not bring the expected economic benefits, leading to an increase in the actual annual value of the operating cost, and a total expected cost higher than that of M1. M2, which does not consider PFR constraints in the planning stage, tends to over-invest in renewable energy.

According to this analysis, the frequency nadir can be guaranteed above the threshold under many different scenarios of actual operation in M1, because this method takes into account PFR constraints both in planning and in operation. M1 limits the number of wind turbines to be built to 356, and constructs one B thermal generator. The purpose of establishing the thermal generator is to ensure that the system has sufficient PFR provision. Type B is chosen because it has significant advantages over other thermal power generators in terms of construction and operating costs. The wind-power accommodation rate of M1 is 5.59% higher than that of M2, and the total cost is reduced by 4.35 M$. Thus, by considering PFR constraints in the planning stage, M1 avoids excessive investment in wind power and ensures optimality in planning for the expansion of the power system.

4.3 Sensitivity analysis

We assume that the inertia time constant of wind turbines is almost zero, and that primary reserves cannot be provided by them for PFR. In a given power-generation plan, the larger the inertia time constant of each thermal generator is, the more adequate the PFR delivery of the system will be, thus allowing more wind power access.

As shown in Fig. 6, the annual total cost decreases by 17.10% (from 514.06 M$ to 426.18 M$) when the inertia constant of thermal units increases from 4.5 s to 7 s. From the perspective of wind-power scale-planning, the overall growth comes in the form of steps. In different stepped phases, the system operators carry out different thermal-generation construction plans; in the same step, thermal power units of the same type are built. The descent-slope period in a step is mainly limited by the maximum primary reserve ratio of unit nominal capacity; the platform period is mainly affected by unit commitment. For instance, when H increases from 5.68 s to 6.09 s, the construction scale

of wind power decreases, because the primary reserves provided for the governors are not adequate in this stage. In this descent-slope period, more wind-power construction can balance a larger part of the load demand in the operation stage, so adequate primary reserves from thermal generators can be set aside for PFR. In the platform period, mainly influenced by SCUC, there is no need to invest in additional wind power: coordinating the output of thermal generators and existing wind generators can ensure the stable operation of the system.

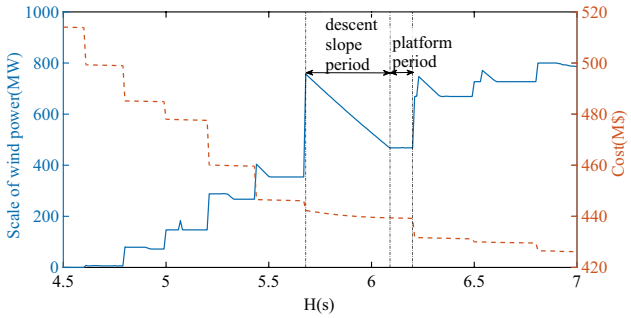

Fig. 6 Wind power construction scale and annual total cost with the increase in the inertia constant *H* of thermal units

From Fig. 7, with the increase of H, the total cost of generation-expansion planning can be gradually reduced. During the stepped-part phase, when thermal generators of the same type are planned, increasing H is conducive to satisfying PFR constraints. More wind-power penetration will force the thermal generators to shut down, so wind-power investment should be reduced or stay the same to ensure PFR adequacy. The general trend, illustrated in Fig. 7, is that, as the basic inertia of the system increases, so does the degree of allowable connection to wind power. Therefore, choosing a thermal unit with a higher inertia constant enhances the primary frequency response.

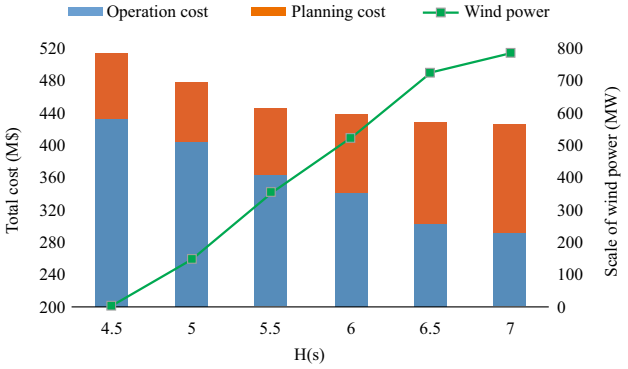

Fig. 7 General trend of wind power construction scale and annual total cost with the increase in the inertia constant H

5 Conclusion

In this paper, an optimal generation-expansion planning framework is proposed that considers primary frequency response. The essential requirement for incorporating PFR constraints during the expansion-planning stage has been formulated as a set of MILP constraints. Case studies based on the modified IEEE 39-bus system demonstrate: (1) A more cost-effective planning strategy can be achieved by considering PFR constraints in the planning stage. When making generation-planning decisions, the expansion of renewable and conventional generation should be coordinated, so that the wind-power accommodation rate can be improved. (2) Selecting units with a higher inertia constant and setting a higher maximum primary reserve ratio help to ensure that sufficient PFR capacity is available for system regulation. These measures can reduce the frequency deviation during failure and facilitate access to more renewable energy.

Appendix

The constraints governing generation-expansion planning in our model are as follows:

(1) Power balance:

$$\sum_{g\in\Phi^{CG}} P^{CG}_{g,s,t} + \sum_{r\in\Phi^{RG}} P^{RG}_{r,s,t} = \sum_{b\in\Phi^{b}} P^{D}_{b,s,t}, \forall s,t. \quad \text{(A1)}$$

Constraints (A1) require that the system load and power balance, where $P^{D}_{b,s,t}$ is the load demand at bus b and Φ^{b} is the set of buses.

(2) Power limit of conventional generators:

$$x_{g,t}P^{CG}_{g,\min} \leqslant P^{CG}_{g,s,t} \leqslant x_{g,t}P^{CG}_{g,\max}, \forall g,s,t, \quad \text{(A2)}$$

$$x_{g,t} \leqslant \alpha^{CG}_{g}, \forall g,t. \quad \text{(A3)}$$

Constraints (A2) and (A3) show the power limits of thermal generators, where $P^{CG}_{g,\min}$ and $P^{CG}_{g,\max}$ are the minimum and maximum power, respectively.

(3) Power limits of renewable generators:

$$0 \leqslant P^{RG}_{r,s,t} \leqslant \alpha^{RG}_{r}P^{RG}_{r,s,t,\max}, \forall r,s,t. \quad \text{(A4)}$$

Constraints (A4) represent the power limit of renewable generator r, where $P^{RG}_{r,s,t,\max}$ is the forecasted power and α^{RG}_{r} indicates whether renewable generator r is included in the construction plans or not.

(4) PFR-related constraints (16)-(23):

The PFR-related constraints are derived in Section 2.

(5) Minimum on/off hours for thermal generators:

$$\sum_{\tau=t}^{t+T_{g,\min}^{On}-1} x_{g,\tau} \geqslant T_{g,\min}^{On} U_{g,t}, \forall g,t, \quad \text{(A5)}$$

$$\sum_{\tau=t}^{t+T_{g,\min}^{Off}-1} \left(1-x_{g,\tau}\right) \geqslant T_{g,\min}^{Off} V_{g,t}, \forall g,t, \quad \text{(A6)}$$

$$U_{g,t}+V_{g,t} \leqslant 1, \forall g,t, \quad \text{(A7)}$$

$$U_{g,t}-V_{g,t} = x_{g,t}-x_{g,t-1}, \forall g,t. \quad \text{(A8)}$$

Constraints (A5) and (A6) enforce thermal generator g to be online or offline for at least $T_{g,\min}^{On}$ or $T_{g,\min}^{Off}$ hours. Constraints (A7) and (A8) describe the relations among the startup, shutdown, and running states of the thermal generators, where $U_{g,t}$ and $V_{g,t}$ are the binary variables for startup and shutdown.

(6) Power flow equations and power limit for lines:

$$P_{l,s,t}^{L} = \sum_{b\in\Phi^{B}} F_{l-b}\left[\sum_{g\in\Phi_{b}^{CG}} P_{g,s,t}^{CG} + \sum_{r\in\Phi_{b}^{RG}} P_{r,s,t}^{RG} - P_{b,s,t}^{D}\right], \forall l,s,t, \quad \text{(A9)}$$

$$-P_{l,\max}^{L} \leqslant P_{l,s,t}^{L} \leqslant P_{l,\max}^{L}, \forall l,s,t. \quad \text{(A10)}$$

The constraints above show the limits of the power flow on the transmission line [30], where $P_{l,s,t}^{L}$ is the transmission power on line l, $P_{l,\max}^{L}$ is the capacity of transmission line l, and $F_{l\text{-}b}$ is the generation shift distribution factor of line l to bus b.

Acknowledgements

This work was supported in part by the National Natural Science Foundation of China (No. U1966204, 51907064).

References

[1] Attya ABT, Hartkopf T (2013) Control and quantification of kinetic energy released by wind farms during power system frequency drops. IET Renewable Power Generation, 7(3): 210-224

[2] Xing P, Shi Q, Wang G et al (2016) Influence analysis of wind power generation on the characteristic of power system frequency. 2016 IEEE 8th International Power Electronics and Motion Control Conference (IPEMC-ECCE Asia), pp. 1444-1447

[3] Rebours YG, Kirschen DS, Trotignon M, Rossignol S (2007) A survey of frequency and voltage control ancillary services—Part I: technical features. IEEE Transactions on Power Systems, 22(1); 350-357

[4] R. J. Koessler, J. W. Feltes, and J. R. Willis (1999) A methodology for management of spinning reserves requirements. Proc. IEEE Power Eng. Soc. Winter Meeting, vol. 1, Feb. 1999, pp. 584-589

[5] Li W, Du P and Lu N (2018) Design of a New Primary Frequency Control Market for Hosting Frequency Response Reserve Offers From Both Generators and Loads. IEEE Transactions on Smart Grid, vol. 9, no. 5, pp. 4883-4892

[6] Li M, McCalley JD (2012) Influence of renewable integration on frequency dynamics. 2012 IEEE Power and Energy Society General Meeting, San Diego, CA, 2012, pp. 1-7

[7] Anderson PM, Mirheydar M (1990) A low-order system frequency response model. IEEE Transactions on Power Systems, 5(3): 720-729

[8] Chávez H., Baldick R, Sharma S (2014) Governor rate-constrained OPF for primary frequency control adequacy. IEEE Transactions on Power Systems, 29(3): 1473-1480

[9] Egido I, Fernandez-Bernal F, Centeno P, Rouco L (2009) Maximum frequency deviation calculation in small isolated power systems. IEEE Transactions on Power Systems, 24(4): 1731-1738

[10] Zhang G, McCalley J (2014) Optimal power flow with primary and secondary frequency constraint. 2014 North American Power Symposium (NAPS), Pullman, WA, 2014, pp. 1-6

[11] Teng F, Trovato V, Strbac G (2016) Stochastic scheduling with inertia-dependent fast frequency response requirements. 2016 IEEE Power and Energy Society General Meeting (PESGM), Boston, MA, 2016, pp. 1557-1566

[12] Kundur P (1994) Power system stability and control. McGraw-Hill, London

[13] B. Porretta and S. Porretta (2018) Calculation of power systems inertia and frequency response. 2018 IEEE Texas Power and Energy Conference (TPEC), College Station, TX, 2018, pp. 1-6

[14] Huang H and Li F (2014) Sensitivity analysis of load-damping, generator inertia and governor speed characteristics in hydraulic power system frequency regulation. 2014 Australasian Universities Power Engineering Conference (AUPEC), Perth, WA, 2014, pp. 1-6

[15] Liao S, Xu J, Sun Y et al (2016) Load-Damping Characteristic Control Method in an Isolated Power System With Industrial Voltage-Sensitive Load. IEEE Transactions on Power Systems, vol. 31, no. 2, pp. 1118-1128

[16] Agüero ED, Colomé DG, Granda NV (2016) Adjustment of frequency transient response with reserve deficit using artificial neural network. 2016 IEEE PES Transmission & Distribution Conference and Exposition-Latin America (PES T&D-LA), Morelia, 2016, pp. 1-6

[17] Zhang G, Ela E and Wang Q (2019) Market Scheduling and Pricing for Primary and Secondary Frequency Reserve. IEEE Transactions on Power Systems, vol. 34, no. 4, pp. 2914-2924

[18] National Grid (2017) Security and Quality of Supply Standards. https://www.nationalgrideso.com/industry-information/codes/security-and-quality-supply-standards/code-documents. Accessed 2 May 2020

[19] Z. Jlassi, K. Ben Kilani, M. Elleuch and C. Bouchoucha (2016) Primary reserves managment in power systems. 2016 13th International Multi-Conference on Systems, Signals & Devices (SSD), Leipzig, 2016, pp. 194-199

[20] You S, Liu Y, Tan J et al (2019) Comparative Assessment of Tactics to Improve Primary Frequency Response Without Curtailing Solar Output in High Photovoltaic Interconnection Grids. IEEE Transactions on Sustainable Energy, vol. 10, no. 2, pp. 718-728
[21] Chengwei F, Xiaoru W, Yufei T, Wencheng W (2017) Minimum frequency estimation of power system considering governor deadbands. IET Generation, Transmission & Distribution, 11(15): 3814-382
[22] S. Mohajeryami, A. R. Neelakantan, I. N. Moghaddam and Z. Salami (2015) Modeling of deadband function of governor model and its effect on frequency Response characteristics. 2015 North American Power Symposium (NAPS), Charlotte, NC, 2015, pp. 1-5
[23] Jlassi Z, Kilani KB, Elleuch M, Bouchoucha C (2016) Primary reserves management in power systems. 2016 13th International Multi-Conference on Systems, Signals & Devices (SSD), Leipzig, 2016, pp. 194-199
[24] Wang J, Zhong H, Wu C et al (2019) Incentivizing distributed energy resource aggregation in energy and capacity markets: An energy sharing scheme and mechanism design. Applied Energy, 252:113471
[25] S. Dehghan, N. Amjady and A. Kazemi (2014) Two-Stage Robust Generation Expansion Planning: A Mixed Integer Linear Programming Model. IEEE Transactions on Power Systems, vol. 29, no. 2, pp. 584-597
[26] A. Zare, C. Y. Chung, N. Safari, S. O. Faried and S. Mahdi Mazhari (2018) A Bi-Level Polyhedral-Based MILP Model for Expansion Planning of Active Distribution Networks Incorporating Distributed Generation. 2018 IEEE Power & Energy Society General Meeting (PESGM), Portland, OR, pp. 1-5
[27] The IBM ILOG CPLEX website (2020) http://www-01.ibm.com/software/websphere/products/optimization/academic-initiative/index.html. Accessed 5 April 2020
[28] Wang J, Qin J, Zhong H et al (2019) Reliability value of distributed solar+ storage systems amidst rare weather events. IEEE Transactions on Smart Grid, 10(4): 4476-4486
[29] PJM Data Directory (2019) PJM wind generation. https://dataminer2.pjm.com. Accessed 23 April 2019
[30] Wang J, Zhong H, Yang Z et al (2019) Incentive mechanism for clearing energy and reserve markets in multi-area power systems. IEEE Transactions on Sustainable Energy

Biographies

Zihan Wang (S'19) received his B.S. degree in Electrical Engineering from North China Electric Power University, Beijing, China, in 2019, where he is currently pursuing his Ph.D. degree. His research interests include renewable power system planning and operation and electricity market.

Jianxiao Wang (S'14-M'19) received his B.S. and Ph.D. degrees in Electrical Engineering from Tsinghua University, Beijing, China, in 2014 and 2019. He was a visiting student researcher at Stanford University, CA, USA. He is currently an assistant professor in the School of Electrical and Electronic Engineering, North China Electric Power University, Beijing, China. He was awarded as the Outstanding Ph.D. Graduate of Tsinghua University, and Junior Fellowships for Advanced Innovation Think-Tank Programming by China Association for Science and Technology. His research interests include multi-energy system planning, electricity market and data analytics.

Gengyin Li (M'03) received his B.S., M.S., and Ph.D. degrees from North China Electric Power University, Beijing, China, in 1984, 1987, and 1996 respectively, all in electrical engineering. Since 1987, he has been teaching in the School of Electrical and Electronic Engineering, North China Electric Power University, where he is currently a Professor. His research interests include HVDC transmission, power quality analysis and control, and emerging transmission and distribution technologies.

Ming Zhou (M'06) received her B.S., M.S., and Ph.D. degrees in electrical engineering from North China Electric Power University, Beijing, China, in 1989, 1992, and 2006, respectively. Since 1992, she has been with the School of Electrical and Electronic Engineering, North China Electric Power University, Beijing, China, where she is currently a Professor. Her research interests include renewable power system planning and operation, electricity market and integrated energy system operation.

(Editor Dawei Wang)